

MAXIMUM POWER WIND EXTRACTION WITH FEEDBACK LINEARIZATION CONTROL APPROACH

SAMIR BELLARBI¹, AHMED BOUFERTELLA¹

Keywords: Feedback linearization control; Wind energy conversion systems; Permanent magnet synchronous generators; Wind turbine; MATLAB; Simulation.

Generally, the permanent magnet synchronous generators model (PMSG) is often used in wind energy conversion systems applications (low to medium power). The PMSG control used in mentoring and induction machine applications has many similarities. It can be controlled in nested speed-torque loops of the synchronous machine via a power electronics converter-specific application. Due to the nonlinearity systems of the wind energy conversion systems (WECS), can be used the feedback linearization control (FLC) to find the optimal solution in the present paper. This approach in WECS, has been applied to energy conversion systems based on grid-synchronous generators.

1. INTRODUCTION

The field of wind energy constitutes an important power technology. 40 years ago, wind technology made several prototypes for industry or research. Over the past decades of technology, today's wind turbines are much more power plants quick to install. However, low wind power has not lost its relevance; nowadays, it is highly interested in power generation, hybrid micro-grid systems, distributed power production, *etc.* Today mature technology still has essential research and development [1].

The variable wind speed control represents a complex problem in the partial load regime, generally aiming at regulating the power harvested from wind by modifying the electrical generator speed, the aim of the control can be to obtain the maximum available power from the wind. For every wind speed, there is a certain rotational speed at which a given wind power curve reaches a maximum (the power factor C_p reaches its maximum value) [2].

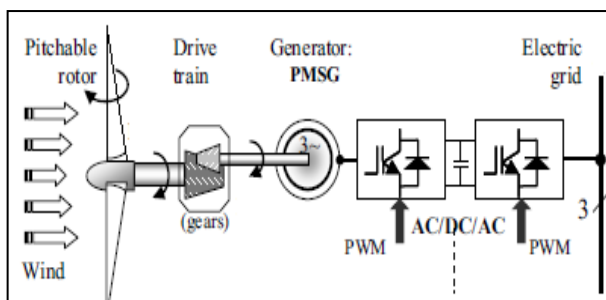


Fig. 1 – Permanent magnet synchronous generators in WECS systems.

There are many studies performed on wind turbines, among these studies are dedicated to synchronous generators, where the advantages consist in the easy maintenance and the low cost. One of the disadvantages of this type of turbine is that it requires complex and more expensive electronic equipment to control its speeds [3–8].

Most of the current research in the wind energy field aims to maximize power point tracking MPPT, its goal to ensure the integrity of the system. This is based on technical data affecting the turbine. Generally, the turbine rotor's technical energetic characteristics are

unknown, but there are estimated rated parameters (power, rotational speed, shaft inertia, *etc.*) are known. Available measurements from the system are the active power and shaft rotational speed generator [9].

Wind energy conversion systems are considered highly nonlinear systems, but with smooth nonlinearity, there may exist perfect solutions for optimal control as feedback linearity control approach FLC. This control method may be suitable for this synchronous generator and is effective in other applications. In wind energy conversion systems case particular, the difficulty in approaching FLC is the synthesis computational complexity, which must use a high-order polynomial function for variation of the wind torque modulus over the tip velocity to capture all operating systems from starting to ensure the steady-state regime, must assume a simplified expression when deciding to use the FLC approach [10–12].

In this paper, the objective is to propose a robust control to achieve better energy performance. It is organized as follows: a general description of the wind energy system. Strategy of feedback linearity control approach and simulation results show the performance of the proposed approach, and finally, a conclusion is deducted. The proposed strategy is compared to the reference value, and traditional PI controllers are confirmed in the MATLAB/Simulink environment. I used this method of control because of:

- Its simplicity is compared to other methods.
- This method is valid for linear systems
- Linear control strategies can be used.
- In this method, we can tune the characteristics of the system.

2. MATHEMATICAL MODELING OF WECS

A. TURBINE MODELING

The wind power generated by the turbine is given by [13]:

$$P_{wr} = \frac{1}{2} C_p \rho \pi R^2 V^3; C_p = 2P_{wr} / \rho \pi R^2 V^3, \quad (1)$$

where P_{wr} is the power of wind captured by the turbine, ρ is the density of air (kg/m^3); R is the radius blade (m), and V is the value of wind speed (m/s).

¹ Centre de développement des énergies renouvelables CDER, BP. 62 Route de l'Observatoire Bouzareah, 16340, Alger, Algérie
E-mail: ac.samirano@gmail.com

The wind power mechanical depends on the power coefficient C_p .

B. PERMANENT MAGNET SYNCHRONOUS GENERATOR MODEL

PMSG model state stator and rotor windings to the d-q axes are given by the following [14]:

$$\begin{cases} \dot{x} = \begin{bmatrix} \frac{R}{L_d + L_s}(-Rx_1 + p(L_q - L_s)x_2\Omega_h) \\ \frac{R}{L_d + L_s}(-Rx_2 + p(L_d + L_s)x_1\Omega_h + p\Phi_m\Omega_h) \end{bmatrix} + \begin{bmatrix} -\frac{1}{L_d + L_s} & 0 \\ 0 & -\frac{1}{L_d + L_s} \end{bmatrix} u, \\ y = \Gamma_G = p\Phi_m x_2, \end{cases} \quad (2)$$

where p is the number of pole pairs; R is the resistance of the stator; L_d, L_q, L_s, d, q are the rotor and the stator inductances; Φ_m is the magnetic flux of the magnets.

The electromagnetic torque is:

$$\Gamma_G = -\frac{3}{2} N_p \Phi_f i_{sq}, \quad (3)$$

the mechanical equation for the PMSG is:

$$J \frac{d\Omega_h}{dt} = \Gamma_{mec} - \Gamma_G, \quad (4)$$

where J is the equivalent inertia to the high-speed shaft; Γ_{mec} is the mechanic torque; Ω_h is the rotational speed, and Γ_G is the electromagnetic torque.

3. FEEDBACK LINEARIZATION CONTROL

There is a lot of different geometry for modeling the feedback linearization control. When the wind system operates in the partial load regime, the aim is to maximize power extraction. Equations 2 and 4 present the shaft speed control, and we calculate the Lie derivatives [15]:

$$\begin{cases} \dot{x} = f(x) + g(x)u, \\ y = h(x), \end{cases} \quad (5)$$

where

$$\begin{cases} x = [i_d \ i_q \ \Omega_h]^T, \\ f(x) = \begin{bmatrix} f_1 \\ f_2 \\ f_3 \end{bmatrix} = \begin{bmatrix} \frac{1}{L_d + L_s}(-Rx_1 + p(L_q - L_s)x_2x_3) \\ \frac{1}{L_d + L_s}(-Rx_2 - p(L_d + L_s)x_1x_3 + p\Phi_mx_3) \\ g(x) = [g_1 \ g_2 \ g_3]^T = \begin{bmatrix} -\frac{1}{L_d + L_s}x_1 & -\frac{1}{L_q + L_s}x_2 & 0 \end{bmatrix}^T \end{bmatrix}, \\ u = R_s, \\ h(x) = x_3 = \Omega_h. \end{cases} \quad (6)$$

To calculate the Lie derivatives, we determine the relative system degree:

$$\begin{cases} L_f h(x) = d_1 v^2 + d_2 v x_3 + d_3 x_3^2 - d_4 x_2, \\ L_g L_f h(x) = -d_4 a_3 x_2 \neq 0. \end{cases} \quad (7)$$

Since $L_g L_f^n h(x) \neq 0$, with $n = 1$, the relative system degree is $r = n + 1 = 2$. Only possible a partial linearization. The linearization effects of system dynamics, because that is responsible for the input/output mapping, and the rest of internal dynamics do not influence the input-output mapping. To modeled the system in the normal form, a coordinate transform:

$$\frac{\partial z_3}{\partial x_1} g_1 + \frac{\partial z_3}{\partial x_2} g_2 + \frac{\partial z_3}{\partial x_3} g_3 = \frac{\partial z_3}{\partial x_1} a_3 x_1 + \frac{\partial z_3}{\partial x_2} a_3 x_2 = 0, \quad (8)$$

where $a_3 = -1/(L_d + L_s)$. The condition is complete for

$z_3 = a_3 x_1/x_2$. The coordinate transformation that leads to the partial linearity is:

$$z = \Phi(x_1, x_2, x_3) = \begin{bmatrix} \Phi_1(x_1, x_2, x_3) \\ \Phi_2(x_1, x_2, x_3) \\ \Phi_3(x_1, x_2, x_3) \end{bmatrix}, \quad (9)$$

$$Z = \begin{bmatrix} x_3 \\ d_1 v^2 + d_2 v x_3 + d_3 x_3^2 - d_4 x_2 \\ a_3 \frac{x_1}{x_2} \end{bmatrix}.$$

To calculate the inverse transform, $\phi(x_1, x_2, x_3)$ should not be singular, and verified this approach perform in MATLAB. The coordinates transform is [16]:

$$\begin{cases} z_1 = h(x) = x_3, \\ z_2 = L_f h(x) = d_1 v^2 + d_2 v x_3 + d_3 x_3^2 - d_4 x_2, \\ z_3 = a_3 x_1 / x_2, \end{cases} \quad (10)$$

and the inverse coordinates transform as:

$$\begin{cases} x_1 = a_3 z_3 \frac{d_1 v^2 + d_2 v z_1 + d_3 z_1^2 - z_2}{d_4}, \\ x_2 = \frac{d_1 v^2 + d_2 v z_1 + d_3 z_1^2 - z_2}{d_4}, \\ x_3 = z_1, \end{cases} \quad (11)$$

with $A = d_1 v^2 + d_2 v z_1 + d_3 z_1^2 - z_2$.

The input control is:

$$u = \frac{1}{L_g L_f h(x)} (-L_f^2 h(x) + u_v), \quad (12)$$

where

$$\begin{cases} L_f^2 h(x) = -d_4 f_2 + (d_2 v + 2d_3 x_3) f_3, \\ L_g L_f h(x) = -d_4 a_3 x_2. \end{cases} \quad (13)$$

The control input has a state feedback component, $L_f^2 h(x)$ and $L_g L_f h(x)$ and a component u_v are Lie derivatives, which forces a dynamic linear input/output mapping. The latter is a state feedback control, as shown in Fig. 2 [17]. For ensure zero error in this steady state regime, was added an integrator (Fig. 3).

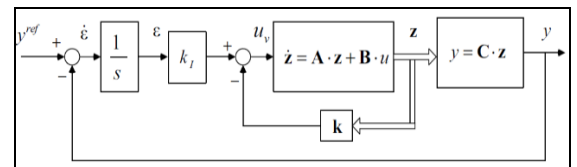


Fig. 2 – State feedback control.

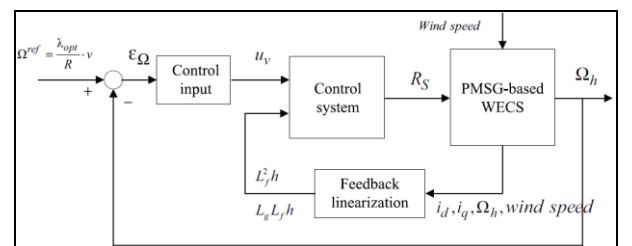


Fig. 3 – Feedback linearization control system.

The linear model is

$$\begin{cases} \begin{bmatrix} \dot{z}_1 \\ \dot{z}_2 \end{bmatrix} = \begin{bmatrix} 0 & 1 \\ 0 & 0 \end{bmatrix} \begin{bmatrix} z_1 \\ z_2 \end{bmatrix} + \begin{bmatrix} 0 \\ 1 \end{bmatrix} u, \\ y = [1 \ 0] \begin{bmatrix} z_1 \\ z_2 \end{bmatrix}. \end{cases} \quad (13)$$

The input u_v is calculated using pole technical allocation $u = k \begin{bmatrix} z_1 \\ z_2 \end{bmatrix} + k_I \varepsilon$, with $u = k \begin{bmatrix} z_1 \\ z_2 \end{bmatrix} + k_I \varepsilon$ and

$$\varepsilon = y^{ref} - y = y^{ref} - [1 \ 0] \begin{bmatrix} z_1 \\ z_2 \end{bmatrix}.$$

Defining the extended state vector $\hat{z} = [z_1 \ z_2 \ \varepsilon]^T$ the linear system is

$$\begin{bmatrix} \dot{z}_1 \\ \dot{z}_2 \\ \dot{\varepsilon} \end{bmatrix} = \begin{bmatrix} 0 & 1 & 0 \\ 0 & 0 & 0 \\ -1 & 0 & 0 \end{bmatrix} \begin{bmatrix} z_1 \\ z_2 \\ \varepsilon \end{bmatrix} + \begin{bmatrix} 0 \\ 1 \\ 0 \end{bmatrix} u + \begin{bmatrix} 0 \\ 0 \\ 1 \end{bmatrix} y^{ref}. \quad (14)$$

The control input, u_v , is obtained as

$$\begin{aligned} & \begin{bmatrix} \dot{z}_1 & \dot{z}_2 & \dot{\varepsilon} \end{bmatrix}^T = \\ & = \begin{pmatrix} \begin{bmatrix} 0 & 1 & 0 \\ 0 & 0 & 0 \\ -1 & 0 & 0 \end{bmatrix} - \begin{bmatrix} 0 \\ 1 \\ 0 \end{bmatrix} [k_1 \ k_2 \ -k_I] \end{pmatrix} \begin{bmatrix} z_1 \\ z_2 \\ \varepsilon \end{bmatrix} + \begin{bmatrix} 0 \\ 0 \\ 1 \end{bmatrix} y^{ref} \end{aligned} \quad (15)$$

$$u_v = -[k_1 \ k_2 \ -k_I] \begin{bmatrix} \dot{z}_1 \\ \dot{z}_2 \\ \dot{\varepsilon} \end{bmatrix}. \quad (16)$$

A closed-loop system is described as mentioned above. k_1 , k_2 , and k_I are calculated using a technical pole placement [18]. Poles pair was defined by the cut-off frequency $\omega_0 = 20$ rad/s and factor the damping $\xi = 0.9$, and $k_1 = 4\ 000$, $k_2 = 136$, $k_I = 40\ 000$.

After the linearization of the system, we use pole placement to the system. When the denominator of the third order transfer function is desired:

$$T(s) = S^3 + 1.75\omega_n S^2 + 2.15\omega_n^2 S + \omega_n^3. \quad (17)$$

The normalized settling time is:

$$\omega_n T_s = 1.04. \quad (18)$$

4. RESULTS AND DISCUSSION

To evaluate the approach control proposed, we used the first simulation, a deterministic reference speed corresponding to wind speeds of 8 to 16 m/s and covering in stages the different operating regimes. The generator speed V_s , the reference optimal speed is shown in Fig. 4. The controller manages to ensure the speed tracking. The power coefficient, the wind turbine power and the active power are shown in Figs. 5, 6, and 7, respectively. Good performance of the system was observed.

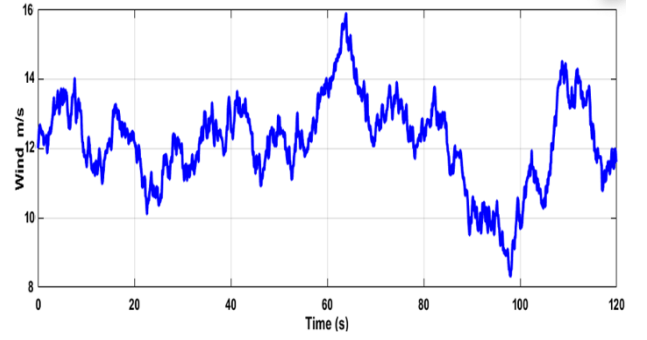


Fig. 4 – Wind speed profile.

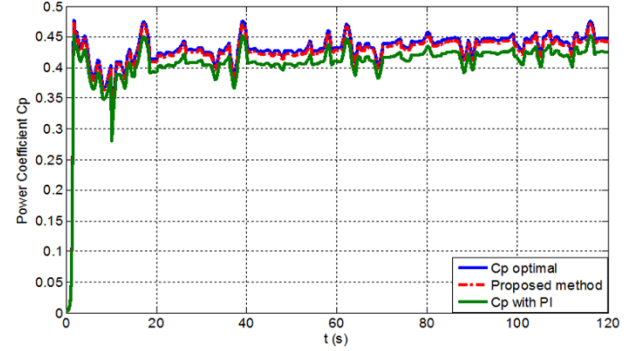


Fig. 5 – Power coefficient profile.

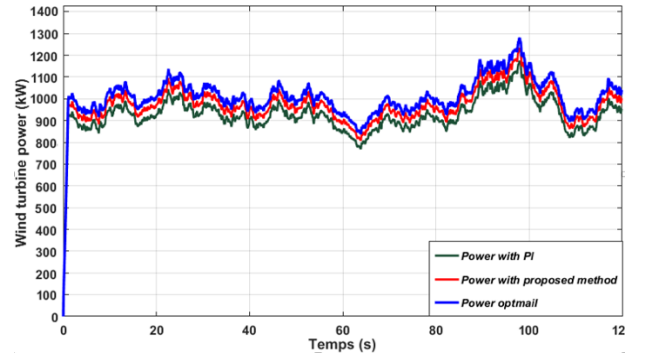


Fig. 6 – Wind turbine power profile.

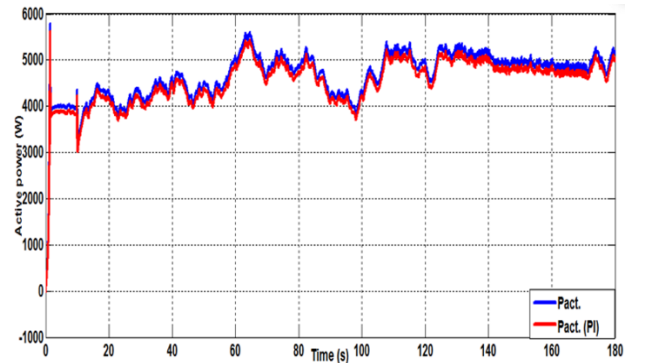


Fig. 7 – Active power profile.

$C_{pmax} = 0.46$ (red), for FLC approach, is almost equal to the value reference 0.48 (blue) represents the power coefficient where it was found equal to 0.44 in the PI controller (green), which shows the good performance of FLC controller.

The active power P is regulated (Fig. 7).

From the results obtained, we can conclude that the FLC controller performs well in tracking power points. This proposed method application can be used in other types of wind energy conversion systems.

5. CONCLUSION

The feedback linearization control method has been tested on a wind power-based permanent magnet synchronous generator. In this case, the exact linearization is possible through the results obtained, and the control algorithm is derived from the partial linearized model. When the wind speed is variable, the results considered have obtained a good closed loop.

The real goal of wind energy systems is to find realistic control and feasible solutions most suitable for an ideal system. We can remark that this choice approach represents the best trade-off between closeness to the targeted optimum on the one hand and simplicity and robustness on the other.

Achieving optimal wind turbine control means that multi-purpose optimization problems must be formulated.

ANNEX

PMSG parameters are: rated power: $P_n = 1.4$ MW; $V = 690$ V and $f = 50$ Hz; stator resistance: $R_s = 0.821$ m Ω ; dq -axis inductances: $L_{dq} = 1.573$ mH;

Number of pole pairs: $N_p = 26$; rated mec. torque: $T_{n, om} = 848.826$ kN·m;

PM flux: $\Phi_f = 5.8264$ Wb.

Received on 11 July 2021

REFERENCES

1. A. Tahri, S. Hassaine, S. Moreau, *Experimental verification of a robust maximum power point tracking control for variable speed wind turbine mechanical sensor*, Rev. Roum. Sci. Techn.–Électrotechn. et Énerg., **64**, 4, pp. 323–330 (2019).
2. D. Saheb Koussa, Y. Bouchahma, M. Koussa, S. Bellarbi, A. Boufertella, *Simulation of a wind generator coupled to a diesel generator*, International Renewable Energy Congress (IREC), 1-6 (2016).
3. M. Szupulski, G. Iwanski, *Synchronization of state-feedback-controlled doubly fed induction generator with the grid*, Bulletin of the Polish Academy of Sciences Technical Sciences **66**, 5 (2018).
4. E. Touti, H. Kraim, R. Pusca, *Modeling of an isolated induction generator considering saturation effect*, Bulletin of the Polish Academy of Sciences Technical Sciences, **67**, 4 (2018).
5. S. Bellarbi, D. Saheb Koussa, *Fuzzy robust control of double-fed asynchronous generator with parameter uncertainties*, Rev. Roum. Sci. Techn.–Électrotechn. et Énerg., **61**, 4, p. 367–371 (2016).
6. S. Bellarbi, D.S. Koussa, A. Djoudi, *Sliding mode control for PMSG-based wind power system*, Journal of Physics: Conf. Series 1081 (2018), 012012.
7. Y. Errami, M. Ouassaid, M., *Sliding mode control scheme of variable speed wind energy conversion system based on the PMSG for utility network connection*, in *Advances and Applications in Sliding Mode Control Systems*, ser. Studies in Computational Intelligence, Springer International Publishing, **576**, pp. 167–200 (2015).
8. A. Asri, Y. Mehoub, S. Hassaine, P. Olivier, *An adaptive fuzzy proportional integral method for maximum power point tracking control of permanent magnet synchronous generator wind energy conversion system*, Rev. Roum. Sci. Techn.–Électrotechn. et Énerg., **63**, 3, p. 320–325 (2018).
9. A. Tahri, S. Hassaine, S. Moreau, *A hybrid active fault-tolerant control scheme for wind energy conversion system based on permanent magnet synchronous generator*, Bulletin of the Polish Academy of Sciences Technical Sciences, **67**, 3 (2018).
10. O. Turksoy, S. Ayasun, Y. Hames, *Computation of robust PI-based pitch controller parameters for large wind turbines*, Canadian Journal of Electrical and Computer Engineering, **43**, 1 (2020).
11. T. Kaczorek, *Global stability of positive standard and fractional nonlinear feedback system*, Bulletin of the Polish Academy of Sciences Technical Sciences, **68**, 2 (2020).
12. Z. Lahlou, Y. Berrada, I. Boumhidi, *Nonlinear feedback control for a complete wind energy conversion system*, International Review of Automatic Control, **12**, 3 (2019).
13. S. Bellarbi, *Analysis and design of wind energy system based on nonlinear speed controller*, Journal of Renewable Energies, **22**, 2, pp. 295–302 (2019).
14. S. Bellarbi, *Optimal estimation and tracking control for a variable-speed wind turbine with PMSG*, Journal of Modern Power Systems and Clean Energy, **8**, 1 (2020).
15. A. Accetta, F. Alonge, M. Cirrincione, *Robust control for high performance induction motor drives based on partial state-feedback linearization*, IEEE Transactions on Industry Applications, **55**, 1 (2019).
16. X. Sun, Z. Jin, Y. Cai, *Grey wolf optimization algorithm based state feedback control for a bearingless permanent magnet synchronous machine*, IEEE Transactions on Power Electronics, **35**, 12 (2020).
17. T. Menara, G. Baggio, D. Bassett, *Conditions for feedback linearization of network systems*, IEEE Control Systems Letters, **4**, 3 (2020).
18. Z. Xiaojian, L. Mingyong, L. Yang, *Impact angle control over composite guidance law based on feedback linearization and finite time control*, Journal of Systems Engineering and Electronics, **29**, 5, pp. 1036–1045 (2018).